Journal of Dental Sciences 20 (2025) 2084–2091

Available online at www.sciencedirect.com

ScienceDirect

journal homepage: www.e-jds.com

Original Article

In vitro evaluation of novel composite bioceramic filaments for alveolar bone regeneration

Yu Ting Li [a], Ju-Hsuan Yang [b,c], Yu-Hsin Chang [b], Hao-Hueng Chang [b,d*], Chun-Pin Lin [b,d**]

[a] *Graduate Institute of Oral Biology, School of Dentistry, National Taiwan University, Taipei, Taiwan*
[b] *Graduate Institute of Clinical Dentistry, School of Dentistry, National Taiwan University, Taipei, Taiwan*
[c] *Far Eastern Memorial Hospital, New Taipei City, Taiwan*
[d] *Department of Dentistry, National Taiwan University Hospital, College of Medicine, National Taiwan University, Taipei, Taiwan*

Received 4 July 2025; Final revision received 9 July 2025
Available online 11 August 2025

KEYWORDS
3D printing;
Bone regeneration;
Composite bioceramic filaments;
Fused deposition modeling;
Polylactic acid;
Tetrahydrofuran

Abstract *Background/purpose:* Alveolar bone defect repair remains a major clinical challenge in oral and maxillofacial reconstruction. This study developed 3D-printable composite filaments combining polylactic acid (PLA) with bioceramic powders and evaluated their physicochemical properties and in vitro osteogenic potential for alveolar bone graft applications.
Materials and methods: Filaments were fabricated via hot processing and tetrahydrofuran (THF) solvent casting, blending PLA with hydroxyapatite (HA) and β-tricalcium phosphate (β-TCP) at a 7:3 ratio. Four groups, H-PLA (heated PLA), H-MIX (heated PLA with HA/β-TCP), T-PLA (THF-processed PLA), and T-MIX (THF-processed PLA with HA/β-TCP) groups, underwent material characterization such as Fourier transform infrared spectroscopy (FTIR), X-ray diffractometer (XRD), scanning electron microscopy (SEM), and compressive strength testing, and MC3T3 cell-based assays for biocompatibility assessment.
Results: H-MIX and T-MIX significantly enhanced compressive strength and osteogenic mineralization compared to PLA-only groups. HA/β-TCP was uniformly dispersed within the PLA matrix. Cell proliferation peaked on day 3, with both composite groups showing higher viability than controls ($P < 0.01$). Alkaline phosphatase (ALP) activity increased by day 7, with T-MIX significantly higher than H-PLA and T-PLA ($P < 0.05$). On day 14, T-MIX and H-MIX showed markedly greater mineralization, with T-MIX displaying the highest calcium deposition ($P < 0.05$ to $P < 0.001$).

* Corresponding author. School of Dentistry, National Taiwan University and National Taiwan University Hospital, No. 1 Changde Street, Taipei, Taiwan.
** Corresponding author. School of Dentistry, National Taiwan University and National Taiwan University Hospital, No. 1, Changde Street, Taipei 10048, Taiwan.
E-mail addresses: changhh@ntu.edu.tw (H.-H. Chang), chunpinlin@gmail.com (C.-P. Lin).

https://doi.org/10.1016/j.jds.2025.07.012

Conclusion: Composite scaffolds made by thermal and solvent casting showed enhanced mechanical strength and osteogenic activity in vitro. T-MIX outperformed other groups in compressive strength, ALP activity, and calcium deposition. These results indicate that HA/β-TCP-reinforced PLA filaments, especially T-MIX, are promising for alveolar bone repair.

Introduction

Alveolar bone regeneration remains a clinical challenge. Although autografts and allografts are widely used, they are associated with notable limitations, such as donor site morbidity, limited availability, and potential immune rejection. The lack of consistent and widely applicable synthetic substitutes continues to hinder the effectiveness of treatment across diverse patient populations (see Figs. 1–4).

Three-dimensional (3D) printing has emerged as a promising method for fabricating customized bone graft substitutes to repair osseous defects. This approach meets patient-specific anatomical needs and reduces the risk of product expiration associated with stockpiled bone substitutes. Among various 3D printing techniques, fused deposition modeling (FDM) is currently one of the most cost-effective and widely adopted methods.[1,2] Polylactic acid (PLA), a biodegradable polymer derived from corn starch, is commonly used as a carrier material and can be compounded with bioceramics to create 3D-printed filaments with high biocompatibility.[3] As 3D printing technology advances, the reconstruction of alveolar bone defects is evolving toward personalized scaffold designs based on the specific size and shape of the defect.[4,5] A common

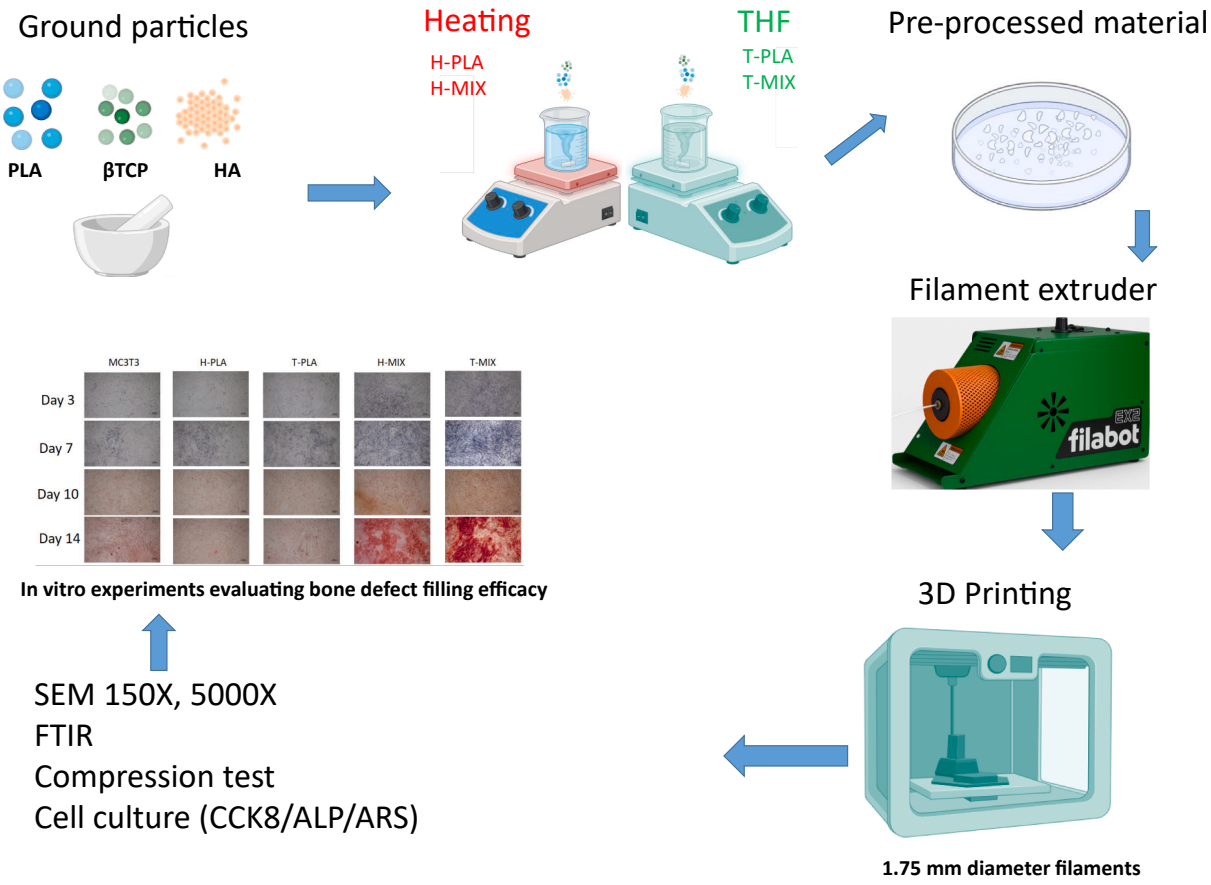

Figure 1 Schematic of material preparation and filament fabrication using hot or tetrahydrofuran (THF)-based processing methods, yielding 1.75 mm diameter filaments, followed by scanning electron microscopy (SEM) (150 × , 5000 ×), Fourier transform infrared spectroscopy (FTIR), mechanical testing, and in vitro assays (CCK8, alkaline phosphatase (ALP), and alizarin red S (ARS)).

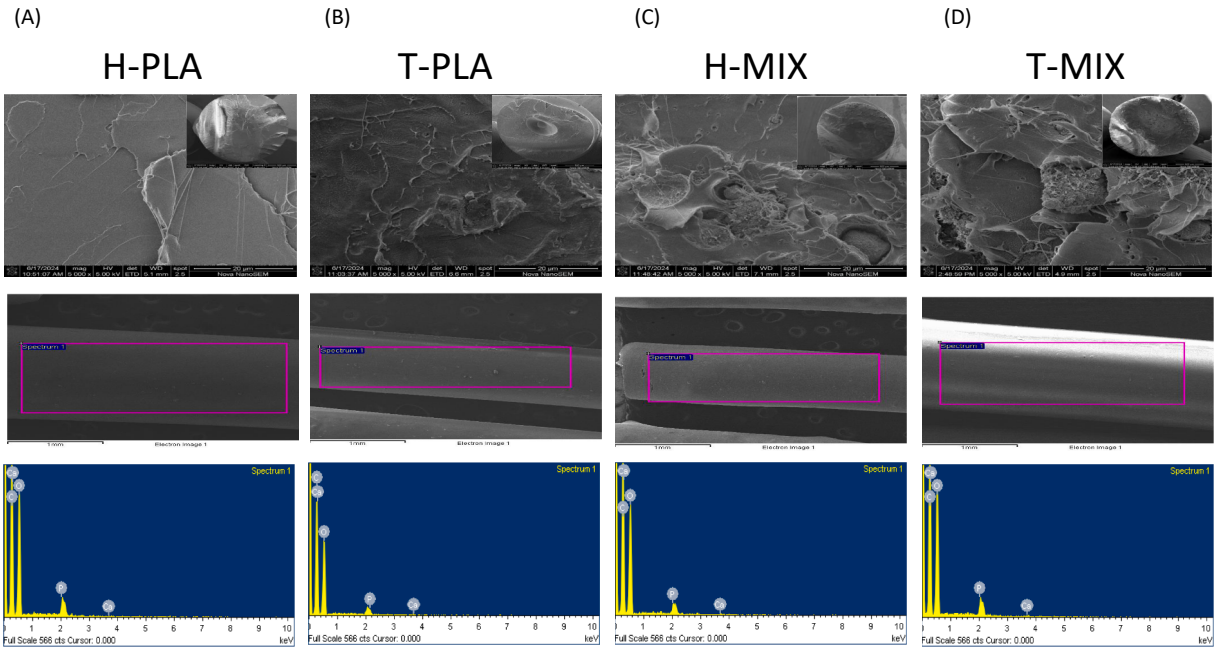

Element	Weight%	Atomic%	Element	Weight%	Atomic%	Element	Weight%	Atomic%	Element	Weight%	Atomic%
C K	48.34	55.49	C K	50.55	57.66	C K	49.95	57.44	C K	48.52	56.15
O K	51.66	44.51	O K	49.45	42.34	O K	48.62	41.98	O K	49.59	43.09
P K	0.00	0.00	P K	0.00	0.00	P K	0.84	0.37	P K	1.01	0.46
Ca K	0.00	0.00	Ca K	0.00	0.00	Ca K	0.59	0.20	Ca K	0.87	0.30
Totals	100.00		Totals	100.00		Totals	100.00		Totals	100.00	

Figure 2 Scanning electron microscopy and energy dispersive X-ray spectroscopy of H-PLA (heated PLA), T-PLA (THF-processed PLA), H-MIX (heated PLA with HA/β-TCP), and T-MIX (THF-processed PLA with HA/β-TCP) filaments showing surface morphology (150 × and 5000 × ; scale bar = 20 μm) and elemental composition.

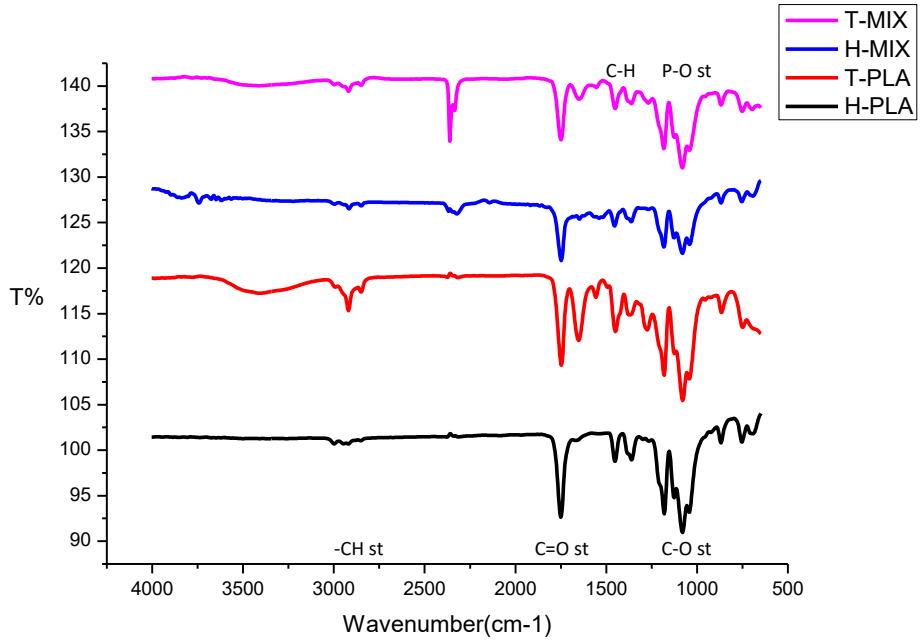

Figure 3 Fourier transform infrared spectra of extruded filaments showing characteristic peaks of polylactic acid (PLA) (H-PLA (heated PLA): black; T-PLA (THF-processed PLA): red) and additional phosphate signals in HA/β-TCP composites (H-MIX (heated PLA with HA/β-TCP): blue; T-MIX (THF-processed PLA with HA/β-TCP): pink).

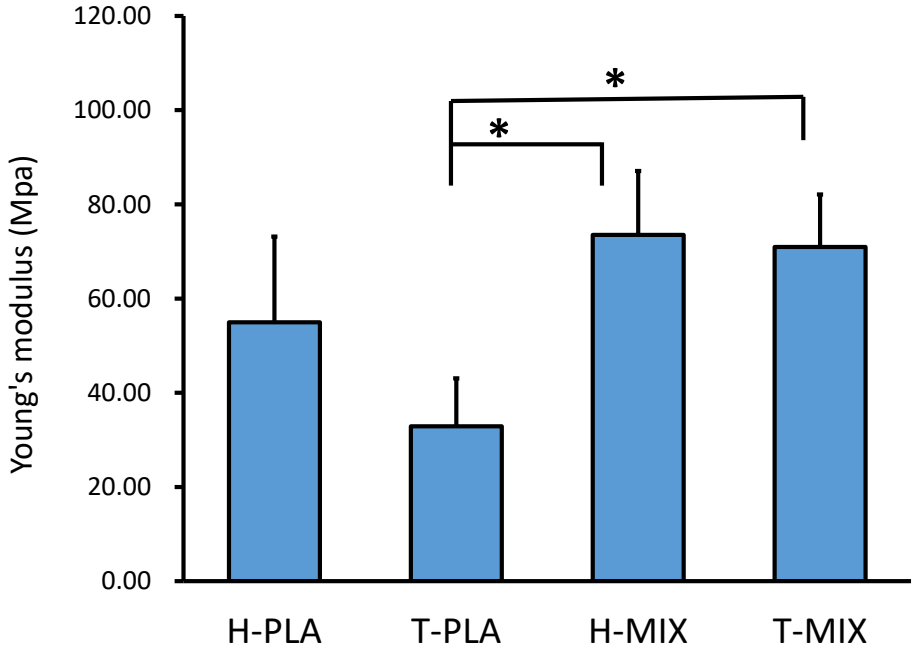

Figure 4 Compressive strength (Young's modulus) of polylactic acid (PLA)-based filaments showing significantly higher values in H-MIX (heated PLA with HA/β-TCP) and T-MIX (THF-processed PLA with HA/β-TCP) groups compared to T-PLA (THF-processed PLA) (*$P < 0.05$), with both exceeding the ISO 5833 threshold of 70 MPa.

strategy involves combining biocompatible polymers with functional additives to enhance mechanical strength and bioactivity. However, conventional processing techniques, such as solvent casting,[6] freeze-drying, and gas foaming,[4,7] often exhibit limited control over pore size and interconnectivity.

In recent years, additive manufacturing has been applied in tissue engineering to precisely control pore architecture and mimic the extracellular matrix, thus facilitating cell attachment and differentiation.[5,7,8] Hydroxyapatite (HA) and β-tricalcium phosphate (β-TCP) are frequently used among various bioceramic materials due to their osteoconductive properties. In addition, solvent-assisted preprocessing is often employed to enhance material homogeneity due to variability in clinical conditions and patient-specific factors. Tetrahydrofuran (THF) is a moderately polar solvent that enables the effective dispersion of ceramic powders within the PLA matrix due to its rapid evaporation and low residual toxicity. It has been widely applied in polymer processing and composite fabrication.[9–12]

Although the use of 3D printing to customize artificial bone scaffolds for patients with alveolar bone defects is gaining traction, the filament formulation remains a subject of considerable debate. No single method of filament fabrication currently meets the needs of all users. In this study, we fabricated composite filaments using both thermal processing and THF-based solvent casting methods, followed by extrusion. The resulting filaments were then evaluated through a series of physicochemical characterizations and in vitro cellular assays to validate their biocompatibility.

Materials and methods

Polylactic acid (PLA) filament fabrication using heating and tetrahydrofuran (THF)-based methods

Before 3D printing, all materials were preprocessed by grinding. PLA was pulverized to an average particle size of approximately 700 μm using a mortar grinder (RM 200, RETSCH GmbH, Haan, Germany) and a centrifugal mill (ZM 300, RETSCH GmbH). HA and β-TCP (Sigma–Aldrich, St. Louis, MO, USA) were ground to approximately 400 nm and 800 nm, respectively.

Composite filaments were fabricated using two processing methods that differed only in the solvent used. The mixed materials were either blended in 100 % ethanol under heat (hot method) or stirred in THF for 24 h. In both protocols, the mixtures were dried in a chemical fume hood for 24 h and subsequently extruded into 1.75 mm filaments using an EX2 filament extruder (Filabot, Barre, VT, USA).

All filaments were printed using FDM with a QTS X160 printer (QTS Technology Co., Zhengzhou, China) at 210 °C nozzle temperature, 0.8 mm nozzle diameter, 0.2 mm layer thickness, and a printing speed of 40–50 mm/s.

Scanning electron microscopy (SEM)

The microstructures of the composite scaffold surface and filaments were observed using a scanning electron microscope (Nova™ NanoSEM 230; Thermo Fisher Scientific, Brno, Czech Republic). Samples were dried, dehydrated, and sputter-coated with gold for 20 s to enhance conductivity.

Images were captured at 150 × and 5000 × magnifications under 5.00 kV accelerating voltage, 7.1 mm working distance, 2.5 spot size, and ETD mode. A representative scale bar of 20 μm is shown.

Fourier transform infrared spectroscopy (FTIR)

FTIR spectroscopy was conducted using a Jasco NIR-4850 spectrometer (JASCO Corporation, Hachioji, Tokyo, Japan). Samples were prepared using the potassium bromide (KBr) pellet method and scanned 15 times per sample over the 400-4000 cm^{-1} wavenumber range, with a resolution of 16 cm^{-1}.

Compressive strength test

Cylindrical specimens (diameter: 4 mm; height: 8 mm) were printed and subjected to compressive testing using a mechanical testing machine (AG-10TE, Shimadzu Corporation, Kyoto, Japan) at a crosshead speed of 1 mm/min. Outliers were excluded from the analysis, and compressive strength was calculated as the mean of three valid replicates. According to ISO 5833, a compressive strength ≥70 MPa is considered acceptable for clinical bone cement applications.

Cell line and biocompatibility assays

The in vitro biocompatibility of the printed scaffolds was evaluated using MC3T3-E1 cells (ATCC, Manassas, VA, USA), a pre-osteoblast cell line derived from mouse calvaria that was widely used in bone tissue engineering studies. Test scaffolds (6 × 6 × 1 mm) were fabricated using both thermal processing and THF-based solvent casting methods. Cell viability and osteogenic potential were assessed using the cell counting Kit-8 (CCK-8; MedChemExpress, distributed by Bio-Genesis Technologies, Inc., Taipei, Taiwan), alkaline phosphatase (ALP) staining, and alizarin red S (ARS) staining.

CCK-8 assay

Cell proliferation and cytotoxicity were assessed using CCK-8. Cells (5 × 10^3 cells/well) were seeded in 96-well plates, and absorbance was measured at 450 nm on days 1, 3, and 7.

Alkaline phosphatase (ALP) assay

Both quantitative and qualitative methods were further used to evaluate ALP activity. For quantitative analysis, cells (1 × 10^4 cells/well) were seeded in 96-well plates and analyzed on days 3 and 7 using an ALP assay kit (GoldBio, St. Louis, MO, USA), with absorbance measured at 405 nm. For qualitative visualization, cells (5 × 10^4 cells/well) were cultured in 24-well plates, fixed with commercial formalin, and stained with 5-bromo-4-chloro-3-indolyl phosphate/nitro-blue tetrazolium (BCIP/NBT, Sigma–Aldrich) according to the manufacturer's protocol. Representative images were captured to visualize ALP-positive regions.

Alizarin red S (ARS) assay

To evaluate the late-stage osteogenesis, calcium deposition was assessed using ARS staining (Santa Cruz Biotechnology).[13] Cells (1 × 10^4/well) were seeded in 96-well plates, and absorbance at 550 nm was measured on days 10 and 14. For qualitative observation, cells (5 × 10^4/well) were seeded in 24-well plates, washed with PBS, fixed with formalin, and stained with ARS. Photographic documentation was performed to examine the formation of calcium nodules.

Results

Scanning electron microscopy (SEM)

SEM revealed that both H-PLA (heated PLA) and T-PLA (THF-processed PLA) groups exhibited smooth laminar surfaces. In contrast, H-MIX (heated PLA with HA/β-TCP) and T-MIX (THF-processed PLA with HA/β-TCP) groups displayed irregular particulate deposits embedded within the PLA matrix, attributed to the HA and β-TCP incorporation. Cross-sectional images showed increased surface roughness and more visible granularity in composite groups. EDS analysis confirmed the presence of only carbon (C) and oxygen (O) in PLA-only groups. At the same time, the composite groups also contained phosphorus (P) and calcium (Ca), verifying successful HA and β-TCP integration.

Fourier transform infrared spectroscopy (FTIR)

All four groups exhibited characteristic absorption peaks of PLA, including the C=O stretching vibration around 1747–1750 cm^{-1} and CH stretching vibrations in the range of 2946–2996 cm^{-1}, which are consistent with the typical spectral features of PLA. Moreover, both H-MIX and T-MIX samples showed phosphate-related PO_4^{3-} absorption bands appearing in the range of approximately 944–1041 cm^{-1}, confirming the presence of HA and β-TCP. These observations agreed with previously published data, supporting the successful integration of PLA with bioceramic components in the fabricated composite filaments.[14–16]

Compressive strength measurement

The compressive strength of T-PLA was the lowest among all groups (32.89 MPa). After adding HA/β-TCP ceramics, both composite groups showed substantial improvements: H-MIX (73.54 MPa) and T-MIX (70.94 MPa). Quantitatively, H-MIX and T-MIX exhibited 2.24- and 2.16-fold increases in compressive strength compared to T-PLA, respectively. These differences were statistically significant ($P = 0.026$ and $P = 0.036$, respectively, Tukey test).

CCK-8 assay

In the cell viability analysis (Fig. 5A), all material groups exhibited an increasing trend in CCK-8 values from day 1 to day 7. A marked proliferation peak was observed on day 3, particularly in the MIX groups containing both HA and TCP.

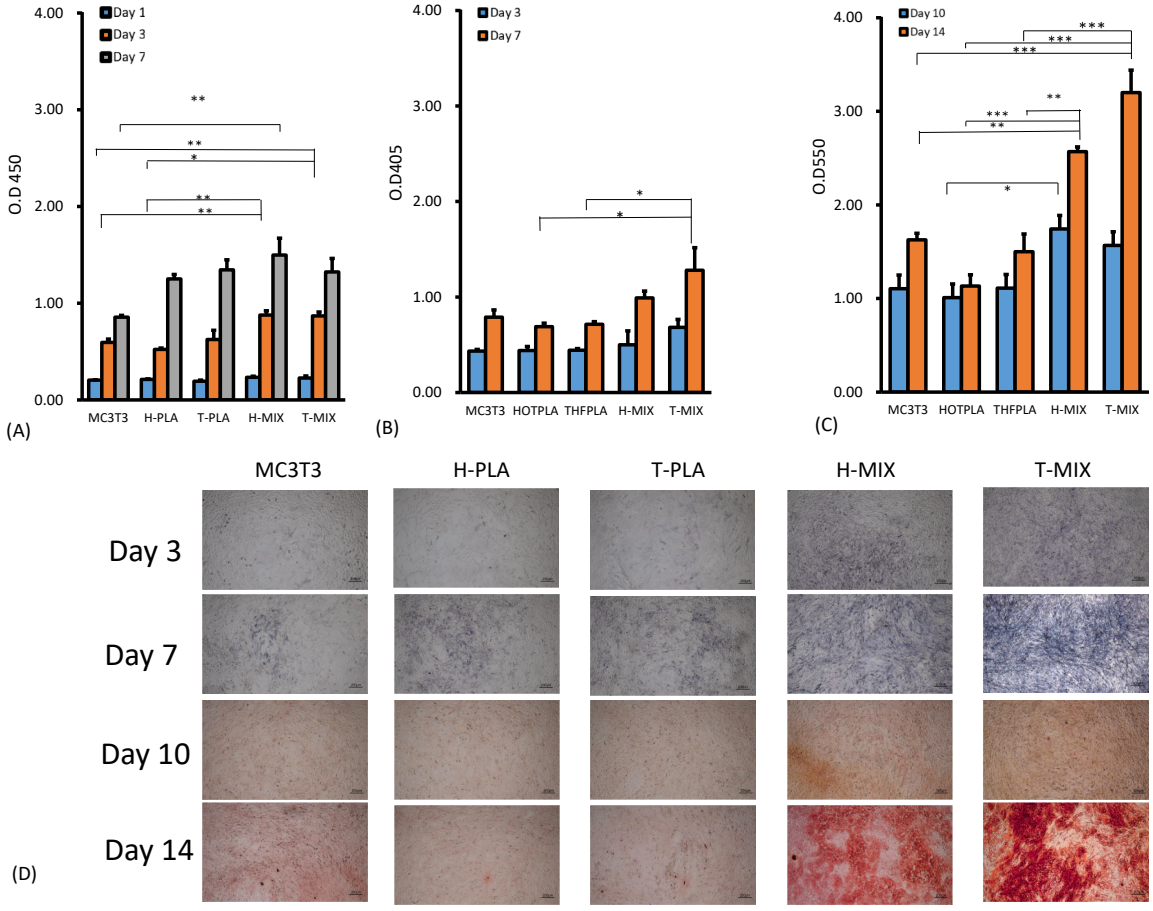

Figure 5 Osteogenic responses of MC3T3-E1 cells on different filaments, including cell proliferation measured by CCK-8 assay on days 1, 3, and 7. (A) Early osteogenic differentiation assessed by alkaline phosphatase (ALP) activity on days 3 and 7. (B) Late-stage mineralization quantified by ARS assay on days 10 and 14. (C) Alizarin red S (ARS)-stained images on days 3, 7, 10, and 14. (D) More intense calcium deposition in H-MIX (heated PLA with HA/β-TCP) and T-MIX (THF-processed PLA with HA/β-TCP) groups, especially on day 14.

These groups showed significantly higher viability than the cell-only and pure PLA groups on day 3 ($P < 0.01$ and $P < 0.05$, respectively), indicating that the osteoinductive effect of the bioceramic powders may stimulate early cell growth. On day 7, H-MIX also revealed a significant difference compared to the MC3T3 control ($P < 0.01$). Notably, all groups demonstrated continuous growth within the 3-day observation period, suggesting that none of the tested materials exhibit cytotoxicity. These results indicate that composites incorporating HA and TCP enhance cell proliferation.

Alkaline phosphatase (ALP) assay

In the ALP assay (Fig. 5B), all groups exhibited increased activity on day 7 compared to day 3. During the early phase of osteogenic induction (day 3), the T-MIX group exhibited a slightly higher ALP level compared to the other groups. By day 7, both H-MIX and T-MIX demonstrated noticeably elevated ALP activity compared to the cell-only and PLA-only groups. Notably, T-MIX showed a statistically significant difference when compared to H-PLA and T-PLA groups ($P < 0.05$), indicating its potential to enhance early osteogenic differentiation. T-MIX exhibited the highest ALP activity among all tested groups. At the same time, H-PLA and T-PLA did not differ significantly from the control, suggesting that the absence of bioceramic fillers may limit osteogenic potential. These findings support the positive effect of HA and TCP incorporation on osteoblast activity.

Alizarin red S (ARS) assay

In the ARS quantification analysis (Fig. 5C), all groups exhibited increased absorbance on day 14 compared to day 10, indicating that the materials support mineralization. Among them, T-MIX displayed the highest level of calcium deposition on day 14, followed by H-MIX. Both MIX groups showed significantly higher mineralization than the MC3T3, H-PLA, and T-PLA groups ($P < 0.05$ to $P < 0.001$), suggesting that the incorporation of HA and TCP effectively enhances the late-stage osteogenesis. The mineralization level in the T-MIX group was approximately two-fold higher than that of the MC3T3 control group. In contrast, H-PLA and T-PLA showed no significant difference from the control group, indicating that pure PLA materials have limited mineralization capacity.

Osteogenic differentiation validated by ALP and ARS staining

In the ALP staining images (Fig. 5D), weak staining was observed across all groups on day 3. However, slightly more intense signals were noted in the H-MIX and T-MIX groups, indicating the initiation of early osteogenic differentiation. By day 7, T-MIX exhibited markedly stronger staining compared to the control and PLA-only groups. At the same time, H-MIX showed broader distribution and increased intensity, suggesting that both composite groups possess notable early osteogenic potential.

To further assess late-stage mineralization, ARS staining was performed. Consistent with these findings, ARS staining results (Fig. 5D) revealed the appearance of red-stained mineralized areas in both MIX groups on day 10. By day 14, T-MIX demonstrated the most prominent staining, with extensive regions of red mineralization, followed by H-MIX. In contrast, the MC3T3 and PLA-only groups showed minimal staining, indicating poor mineralization. These imaging results support the quantitative ARS data and further confirm the late-stage osteogenic potential of HA and TCP-containing composites.

Discussion

In this study, composite bioceramic filaments were successfully fabricated by incorporating HA and β-TCP into a PLA matrix using two different processing methods. The materials exhibited favorable mechanical strength and biocompatibility, supporting their potential as substitutes for alveolar bone grafts. SEM imaging revealed uniform dispersion of ceramic particles within the PLA matrix, while FTIR spectra verified the presence of characteristic absorption bands corresponding to HA, β-TCP, and PLA components. Notably, the compressive strength of the composite groups exceeded the ISO 5833 standard, which specifies a minimum compressive strength of 70 MPa for implantable materials used in oral cavity reconstruction, thereby suggesting their suitability for load-bearing applications in alveolar bone reconstruction. According to the ANOVA and Tukey post hoc test, both H-MIX and T-MIX groups showed statistically significant improvements in compressive strength compared to the T-PLA group ($P < 0.05$), with values approximately 2.24- and 2.16-fold higher. The enhanced performance of the T-MIX group may be attributed to the combined effects of ceramic reinforcement and solvent-assisted microstructural densification.

In contrast, T-PLA exhibited the lowest strength (32.89 MPa), likely due to residual porosity from solvent casting. Similar observations have been reported in the literature for THF-processed PLA materials, which tend to show reduced mechanical performance.[17] This finding suggests that direct molding and densification in our T/PLA process significantly improve mechanical integrity despite using THF.

The biological evaluation further supported the efficacy of the composite scaffolds. H-MIX and T-MIX groups significantly improved the early and late osteogenic differentiation responses. CCK-8 and ALP assays revealed enhanced cell proliferation and the early osteogenic differentiation, while ARS staining demonstrated increased calcium deposition in the later stages of osteogenic differentiation. Among the groups, T-MIX consistently showed superior performance, which may be related to the use of THF during fabrication. THF has been reported to enhance polymer—ceramic dispersion and reduce residue in the composite systems.[9—12]

Notably, the ceramic phase in both H-MIX and T-MIX filaments was prepared using a HA/β-TCP ratio of 30:70, a composition adopted in the previous studies. It is reported to provide a favorable balance between degradation and osteoconductivity.[18] In our research, the T-MIX scaffold, prepared via a THF-assisted method, exhibited enhanced mineralization and osteogenic activity, suggesting that this formulation offers a favorable balance between degradation and osteoconductivity. Additionally, scaffolds with higher TCP content demonstrated increased calcium ion release and favorable mechanical properties, which supported the early-stage bone ingrowth.[19] Therefore, the improved performance observed in H-MIX and T-MIX groups in our study could be attributed to selecting a HA30/TCP70 ceramic phase, which supported the early-stage degradation and osteogenesis. These findings align with the results of the previous reports highlighting the promise of additive manufacturing and PLA-based composite bioceramic scaffolds in regenerative dentistry and offer new comparative insights into different filament fabrication techniques.[5,7,8]

This study demonstrated that PLA-based composites incorporating HA and β-TCP enhance in vitro cell proliferation, osteogenic differentiation, and mineralization. Among all groups, T-MIX filaments prepared via the THF method exhibited the most favorable bioactivity, indicating their potential for bone tissue engineering. However, as this study was limited to in vitro assessments, further in vivo validation is required to confirm the clinical applicability.

Declaration of competing interest

The authors have no conflicts of interest relevant to this article.

Acknowledgments

This study was supported by the National Taiwan University Hospital grant (NTUH.113-S0015) and Far Eastern Memorial Hospital grant (FEMH 110-2314-B-418-003-MY2 2/2).

References

1. Mazzanti V, Malagutti L, Mollica F. FDM 3D printing of polymers containing natural fillers: a review of their mechanical properties. *J Polym* 2019;11:1094.
2. Bharadwaz A, Jayasuriya AC. Recent trends in the application of widely used natural and synthetic polymer nanocomposites in bone tissue regeneration. *Mater Sci Eng* 2020;110:110698.
3. Singhvi M, Gokhale D. Biomass to biodegradable polymer (PLA). *RSC Adv* 2013;3:13558—68.
4. Bártolo PJ, Domingos M, Patrício T, Cometa S, Mironov V. Biofabrication strategies for tissue engineering. In: Bártolo PJ,

Bidanda B, eds. *Advances on modeling in tissue engineering. Boston*; 2011:137—76.
5. Melchels FP, Domingos MA, Klein TJ, Malda J, Bartolo PJ, Hutmacher DW. Additive manufacturing of tissues and organs. *Adv Polym Sci* 2012;37:1079—104.
6. Prasad A, Sankar MR, Katiyar V. State of art on solvent casting particulate leaching method for orthopedic scaffolds fabrication. *Materialia* 2017;4:898—907.
7. Yeong WY, Chua CK, Leong KF, Chandrasekaran M. Rapid prototyping in tissue engineering: challenges and potential. *Trends Biotechnol* 2004;22:643—52.
8. Bartolo P, Domingos M, Gloria A, Ciurana J. BioCell printing: integrated automated assembly system for tissue engineering constructs. *CIRP Ann* 2011;60:271—4.
9. Kim Y, Lee EJ, Davydov AV, et al. Biofabrication of 3D printed hydroxyapatite composite scaffolds for bone regeneration. *Biomed Mater* 2021;16:045002.
10. Prasopthum A, Shakesheff KM, Yang J. Direct three-dimensional printing of polymeric scaffolds with nanofibrous topography. *Biofabrication* 2018;10:025002.
11. Jayakumar N, Arumugam H, Albert Selvaraj AD. Mechanical behaviour of the post processed 3D printed PLA parts using polar and non-polar solvents. *Polym Bull* 2024;81:4257—74.
12. Tallia F, Russo L, Li S, et al. Bouncing and 3D printable hybrids with self-healing properties. *Mater Horiz* 2018;5:849—60.
13. Rashidi N, Najmoddin N, Tavakoli AH, Samanipour R. 3D printed hetero-layered composite scaffold with engineered superficial zone promotes osteogenic differentiation of pre-osteoblast MC3T3-E1 cells. *Surf Interfaces* 2024;51:104683.
14. Olam M, Tosun N. 3D-printed polylactide/hydroxyapatite/titania composite filaments. *Mater Chem Phys* 2022;276:125267.
15. Wu D, Spanou A, Diez-Escudero A, Persson C. 3D-printed PLA/HA composite structures as synthetic trabecular bone: a feasibility study using fused deposition modeling. *J Mech Behav Biomed Mater* 2020;103:103608.
16. Xidaki D, Agrafioti P, Diomatari D, et al. Synthesis of hydroxyapatite, β-tricalcium phosphate and biphasic calcium phosphate particles to act as local delivery carriers of curcumin: loading, release and in vitro studies. *Materials* 2018;11:595.
17. Önder ÖC, Yilgör E, Yilgör I. Fabrication of rigid poly (lactic acid) foams via thermally induced phase separation. *Polymer* 2016;107:240—8.
18. Shao CS, Chen LJ, Tang RM, Zhang B, Tang JJ, Ma WN. Degradation and biological performance of porous osteomimetic biphasic calcium phosphate in vitro and in vivo. *Rare Met* 2022;41:1478—89.
19. Zerankeshi MM, Mofakhami S, Salahinejad E. 3D porous HA/TCP composite scaffolds for bone tissue engineering. *Ceram Int* 2022;48:22647—63.